



Boron nitride and hyperbranched polyamide assembled recyclable polyisoprene vitrimer with robust mechanical properties, high thermal conductivity and remoldability

Lingyun Huang^{a,b}, Yinxin Yang^{a,b}, Ruiyao Wu^{a,b}, Weifeng Fan^a, Quanquan Dai^a, Jianyun He^{a,*}, Chenxi Bai^{a,b,*}

^a Key Laboratory of High-Performance Synthetic Rubber and its Composite Materials, Changchun Institute of Applied Chemistry, Chinese Academy of Sciences, Changchun, 130022, China

^b University of Science and Technology of China, 230026, Hefei, Anhui, China

ARTICLE INFO

Keywords:

Vitrimer
Boron nitride
Exchangeable bond
Thermal conductivity
Recyclability

ABSTRACT

Rubber has huge potential applications for thermal management due to its outstanding softness and elasticity, however, its low thermal conductivity limits its applications, and the vulcanized rubber also has the problem of being unrecoverable. Therefore, the development of recyclable rubber-based material with good mechanical properties, high thermal conductivity remains a challenge. Herein, the dynamic β -hydroxyl ester bonds were introduced into the composites of the epoxidized boron nitride (EBN) and the epoxidized polyisoprene (EPI) matrix via carboxyl-terminated hyperbranched polyamide (HBPA), forming dynamic covalently cross-linking rubber-based vitrimers. The covalent-bonds-mediated interface reduces the phonon scattering and enables the material to have a relatively high thermal conductivity of 0.51 W/mK under a loading of 50 phr (parts per one hundred parts of rubber) of EBN. In addition, the introduction of exchangeable bonds brings the materials the capability to change the network topology at high temperatures, exhibiting excellent recyclability and remoldability.

1. Introduction

Recently, the rapid development of electronics poses higher challenges for heat dissipation [1,2]. The heat accumulation will reduce the lifetime and reliability of devices [3]. In response to this problem, thermal management materials have attracted much attention [4,5]. Traditional polymer-based materials are widely used in thermal management materials for their excellent processing performance, light weight, and electrical insulation [6,7]. Among them, the high softness and high elasticity of rubber make it easily deformed under pressure to fill the gaps of the mating surface, which has great potential applications in thermal interface materials (TIM). However, the further applications of rubber are limited by its inherent low thermal conductivity. In addition, traditional rubber products must be vulcanized to have good mechanical properties and high elasticity, which often makes the

materials unrecyclable, causing environmental pollution and waste of resources [8]. Hence, the development of rubber-based composites with robust mechanical properties, high thermal conductivity and recyclability is of great significance for practical applications in aerospace and electronic fields.

Various studies have proved that the addition of thermally conductive fillers can effectively improve the thermal conductivity of polymers [9,10]. Traditional low-cost thermal conductive fillers like zinc oxide (ZnO) [11], aluminum oxide (Al_2O_3) [12], silicon carbide (SiC) [13], silicon nitride (Si_3N_4) [14] and aluminum nitride (AlN) [15] were widely used. However, in order to establish a thermally conductive network, it is often necessary to increase the loading fraction of fillers, which makes processing difficult and reduces mechanical properties [16]. Carbon nanotubes [17], graphene [18] and other carbon materials have high thermal conductivity, but their excellent electrical

* Corresponding author. Key Laboratory of High-Performance Synthetic Rubber and its Composite Materials, Changchun Institute of Applied Chemistry, Chinese Academy of Sciences, Changchun 130022, China. .

** Corresponding author. Key Laboratory of High-Performance Synthetic Rubber and its Composite Materials, Changchun Institute of Applied Chemistry, Chinese Academy of Sciences, Changchun 130022, China.

E-mail addresses: jyhe@ciac.ac.cn (J. He), baicx@ciac.ac.cn (C. Bai).

<https://doi.org/10.1016/j.polymer.2020.122964>

Received 10 June 2020; Received in revised form 8 August 2020; Accepted 14 August 2020

Available online 27 August 2020

0032-3861/© 2020 Elsevier Ltd. All rights reserved.

conductivity also limits their application in thermal management materials. Boron nitride platelets attracted much attention in thermal management for their similar structure to graphene, high thermal conductivity, low dielectric constant and high breakdown strength [19,20]. Gu et al. [21] prepared high-thermal-conductivity composites by kneading hexagonal boron nitride and polymethyl-vinyl siloxane rubber and then hot-pressing, which proved that high loading fraction of boron nitride can effectively improve the thermal conductivity of the composites. However, the aggregation of hexagonal boron nitride (hBN) led to uneven distribution and reduced enhancement efficiency. Covalent or non-covalent surface modifications of boron nitride are beneficial to the improvement of the thermal conductivity of polymers because of the enhanced interaction between fillers and matrix [22]. Takuya et al. [23] exfoliated and noncovalently functionalized boron nitride with ionic liquid. A composite film of modified boron nitride and polymethyl methacrylate was prepared. The composites exhibits high thermal conductivity ($7.3 \text{ W m}^{-1} \text{ K}^{-1}$), which is attributed to good dispersion of boron nitride and strong interfacial interaction. Kim et al. [24] incorporated boron nitride into epoxy butadiene by grafting 3-glycidypropyl-trimethoxysilane and 3-chloropropyltrimethoxy-silane. The thermal conductivity of composite was increased by 40% compared with the unmodified boron nitride under the same loading. Compared with plenty of researches of high thermal conductive BN/rubber composites, however, the BN-based rubber materials featuring recyclability attracted less research attention. The network in traditional vulcanized rubber is irreversible, which hinders the recycling of products, placing a huge burden on the environment and greatly reducing the service life of the TIM.

Recently, amounts of methods have been developed to produce high mechanical strength elastomer with recyclability and reprocessing performance by introducing dynamic covalent bond [25]. Leibler and colleagues introduced the concept of vitrimers [26]. Vitrimers can change the cross-linking network topology through thermally-triggered exchange reactions, in which the amount of dynamic covalent bonds and cross-linking density remain constant during network rearrangement, and the viscosity is depend on the exchange reaction rate, following Arrhenius's law [27,28]. In other words, vitrimers behave as cross-linking polymers at ambient temperature, but can be quickly reshaped and recycled at the exchange temperature. Based on this feature, vitrimers have many fascinating features such as recyclability, reprocessing and self-healing properties. A variety of vitrimers with different types of exchange bonds have been developed, including carboxylic acid ester exchange [29], disulfide exchange [30], trans-alkylation [31], olefin metathesis [32], imine bond exchange [33], borate exchange [34], oxime carbamate ester exchange [35], siloxane silanol exchange [36], etc. Yang et al. [37] introduced carboxylic acid ester exchange reactions into a thiol-epoxy BN/elastomer to prepare

high thermal conductive composites with self-healing capability and recyclability. The high loading of BN increases the thermal conductivity but also destroys the continuous structure of polymer and reduces the mechanical properties. So far, the method of manufacturing BN-based elastomer with high mechanical properties, high thermal conductivity and recyclable performance by dynamic exchange bonds remains to be explored.

Hyperbranched polymers (HBPs) have the characteristics of low viscosity, high functionality, and high solubility, which can be used as either non-reactive modifiers or reactive modifiers. Phase separation inevitably occurs if HBPs acted as non-reactive modifiers, accompanied by a decrease in glass transition temperature (T_g) and tensile strength [38]. However, a homogeneous network can be obtained if HBPs acted as **reactive** modifiers.. In this work, we introduced carboxyl-terminated HBPA into the EBN/EPI cross-linking network and synthesized a kind of robust elastomeric vitrimer composites, with high thermal conductivity, recyclability and remoldability (Fig. 1). Under the action of catalysts, carboxyl groups on HBPA can react with epoxy groups on the EBN and EPI, forming β -hydroxyester bonds to obtain covalently cross-linking elastomer. With the transesterification reaction of β -hydroxyester bonds, the network topology can be changed at high temperatures to achieve reprocessing, recyclability and remoldability. In addition, EBN can be well dispersed in the matrix through interfacial covalent bonds, which reduces phonon scattering and improves the thermal conductivity and mechanical properties of EPI composites. Besides, considering the huge annual consumption of isoprene rubber, this research also provides a sustainable method for the recycling of cross-linking waste rubber materials.

2. Experimental section

2.1. Materials

Cis-1,4- Polyisoprene (PI, *cis*-1,4 content = 98%, $M_n = 2 \times 10^5$, $M_w/M_n = 1.67$) was obtained from Dushanzi Petrochemical Company, PetroChina. Hexagonal boron nitride (hBN) with an average diameter of 1–2 μm were purchased from Shanghai Macklin Biochemical Co. (China). 3-Chloroperoxybenzoic acid (mCPBA), γ -(2,3-epoxypropoxy) propyltrimethoxysilane (KH-560), 5-Aminoisophthalic acid (5-AIPA), 1,5,7-Triazabicyclo [4.4.0]dec-5-ene (TBD, 98%) and 1,2-dimethylimidazole (DMI, 99%) were purchased from Sigma-Aldrich.

2.2. Preparation of composites

2.2.1. Preparation of EPI

10 g of PI was dissolved in dichloromethane and stirred at 25 °C until completely dissolved. Then 3 g of mCPBA in dichloromethane was

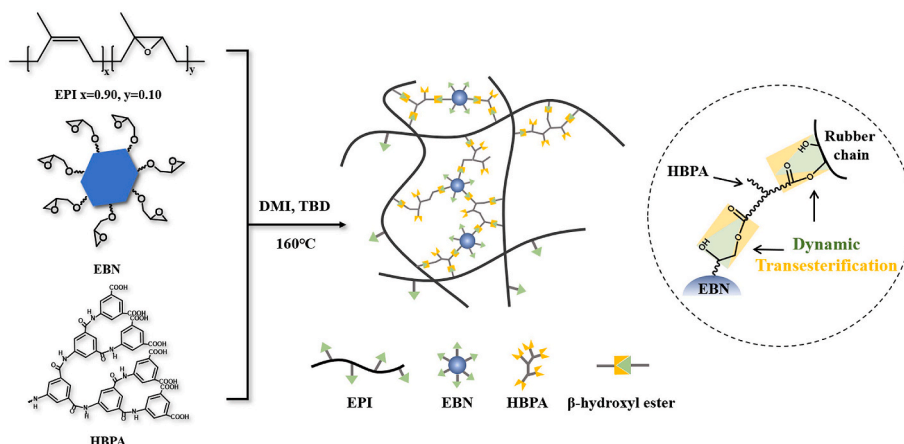


Fig. 1. Fabrication of EB nanocomposites based on β -hydroxyl ester bonds.

dropped at 0 °C. Products were precipitated with methanol after 3 h and dried under vacuum until constant weight. The content of epoxy group in EPI (E_{epo}) was calculated from the intensity ratio of the signals at 2.7 and 5.1 ppm in ^1H NMR spectra, as in the following equation:

$$E_{epo} = \frac{I_{2.7}}{I_{2.7} + I_{5.12}} \times 100\% \quad (1)$$

The degree of epoxidation calculated by ^1H NMR is 10% (Fig. S1).

2.2.2. Preparation of EBN

The preparation of hydroxylated boron nitride (BN-OH) was prepared according to the literature description [39]. 1 g of hBN were suspended in 100 ml of 5 mol/L sodium hydroxide solution, stirred at 120 °C for 48 h, and then filtered. Wash the products with ultrapure water until the pH change to 7. The obtained hydroxylated boron nitride was dried under vacuum at 90 °C for 24 h.

An appropriate amount of KH-560 (5 wt% of the BN-OH) were added into deionized water at 50 °C and stirred for 60 min, and then 1 g BN-OH were added into system and stirred at 80 °C for 1 h. The EBN was washed with deionized water and dried under vacuum at 90 °C until constant weight.

2.2.3. Preparation of HBPA

In a typical experiment, 5 g of 5-AIPA was dissolved in 100 ml of *N*-methyl pyrrolidone, followed by adding 25 ml of pyridine and 26 ml of triphenylphosphine. The system reacted at 100 °C for 3 h under N_2 atmosphere. After that, products were precipitated and washed with cold methanol. The product was dried to constant weight in a vacuum oven at 90 °C.

In order to compare the effect of polyamide structure on material properties, a linear structure of polyhexamethylene adipate (PA-66), hyperbranched aliphatic polyamide (HBP-aliphatic) and amino-terminal hyperbranched aromatic polyamide (HBP-NH₂) were synthesized according to the literature [40–42].

2.2.4. Preparation of EB composites

The required amounts of EPI, EBN, HBPA, DMI and TBD were mixed on double-roll open mill. The mixture was compression molded at 160 °C for 30 min. The content of EBN was controlled to be 10, 20, 30, 40, 50 phr (parts per one hundred parts of rubber). The content of HBPA was controlled to 10 phr. The DMI and TBD loadings were 3.7 phr and 1 phr, respectively. TBD was used to catalyze the subsequent transesterification reactions, and DMI was used to promote the esterification. Composites were represented as EBx, where x represented x phr EBN.

2.3. Characterization

Details of structure and performance characterization in this article are given in **Supplementary Information S1**.

3. Results and discussion

3.1. Formation of covalent cross-linking networks

Silane coupling agents were usually used to modify BN to improve dispersibility and enhance the interaction between rubber and BN [43]. Herein, EBN was prepared by grafting KH-560 to hydroxylated boron

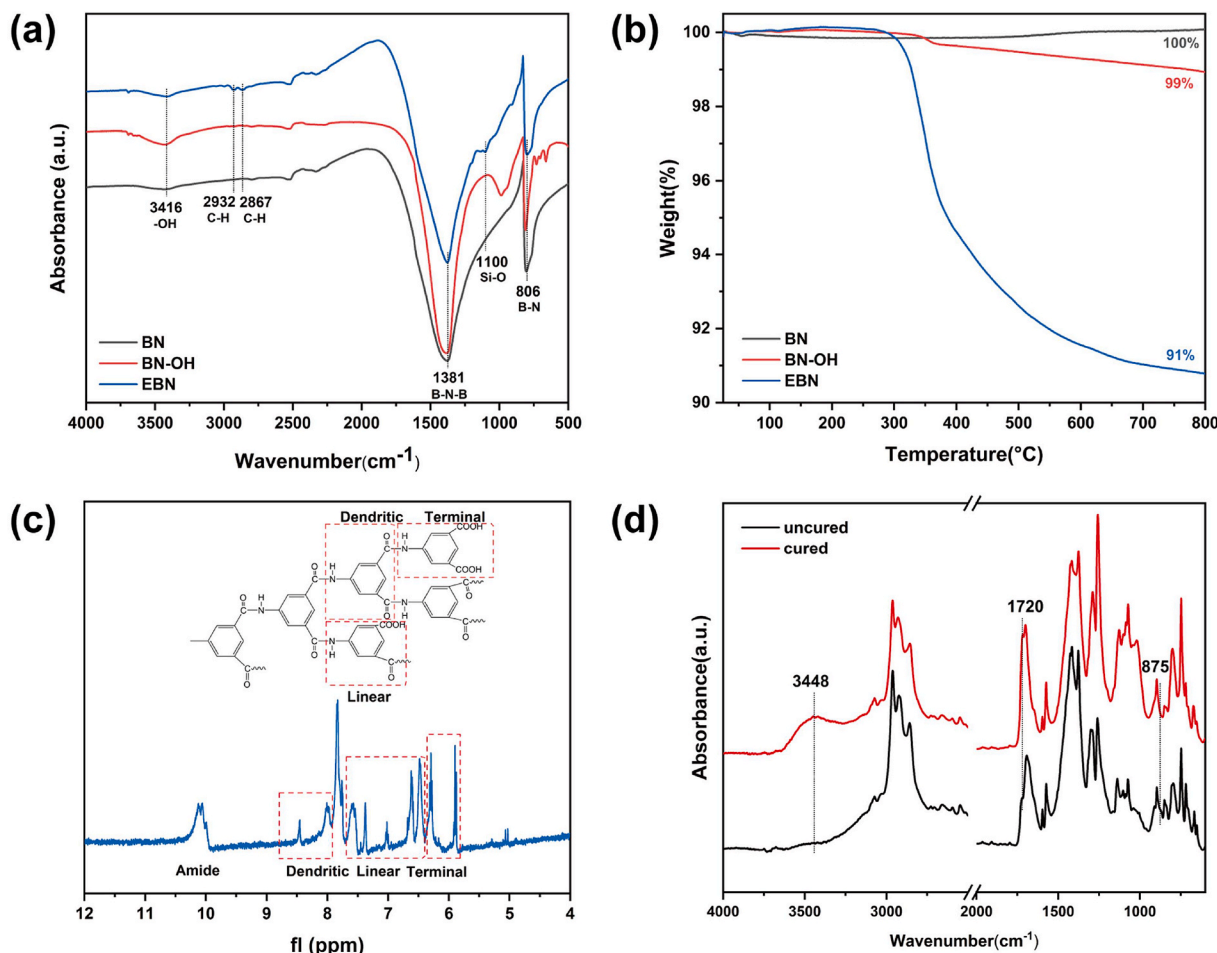


Fig. 2. (a) FTIR spectra and (b) TGA curves of BN, BN-OH and EBN. (c) ^1H NMR spectra of HBPA. (d) FTIR spectra of uncured and cured EB20.

nitride (BN-OH). The FTIR spectra of BN, BN-OH, and EBN was shown in Fig. 2a. The peaks at 1381 cm^{-1} and 806 cm^{-1} for BN can be corresponded to the B-N-B bending and the B-N stretching, respectively. For BN-OH, the enhanced peak at 3416 cm^{-1} is related to the stretching vibration of B-OH [39]. By comparing the XRD spectra of hBN and BN-OH in Fig. S2, it can be found that the (002) peak of BN-OH was sharper than that of BN, which means the (002) crystal faces of BN-OH are exposed more than in hBN, and the BN-OH may be exfoliated along the (002) crystal faces without destroying its crystalline structure. Two peaks at 2932 and 2867 cm^{-1} for EBN in Fig. 2a are corresponded to the stretching vibration of -CH- in KH-560. And the peak at 1100 cm^{-1} relates to the stretching vibration of the Si-O-Si in KH-560 [24]. These results indicated KH-560 has been grafted onto BN-OH successfully. As can be seen from the SEM image of Fig. S3, EBN has changed little compared to hBN except for the reduction in particle size, showing that the modification did not affect the structure of BN. The grafting amount of KH-560 on BN-OH surface was estimated by TGA. As Fig. 2b shows, weight loss was not observed for BN. BN-OH exhibit 1 wt% loss at $800\text{ }^{\circ}\text{C}$, which was attributed to the loss of -OH on the surface. About 9 wt% loss of EBN can be attributed to the decomposition of the KH-560. The graft density was calculated to be 0.419 mmol/g according to the formula (Supplementary Information S1Eq (1)).

The carboxyl-terminated HBPA was prepared through self-condensation of 5-AIPA. Fig. 2c shows the ^1H NMR spectrum of HBPA. The structure of HBPA includes linear, dendritic and terminal units, which correspond to three types of aromatic proton peaks. The peaks at $8.5\text{--}7.8\text{ ppm}$; $7.3\text{--}6.6\text{ ppm}$ and $6.3\text{--}5.9\text{ ppm}$ are corresponded to the aromatic protons of the dendritic units, linear units and terminal units, respectively. Moreover, the peaks at $10.6\text{--}9.8\text{ ppm}$ correspond to the amide groups [41]. FTIR spectrum (Fig. S4) also shows that HBPA was successfully prepared. The degree of branching of HBPA (DB) is calculated according to Fréchet's formula [44]:

$$DB = \frac{D + T}{D + T + L} \quad (2)$$

D, L and T represent the peak areas integration ratio of dendritic unit (D), linear unit (L) and terminal unit (T), respectively. And the content of carboxyl groups per molecule (N_{COOH}) can be estimated according to the following formula [41]:

$$N_{\text{COOH}} = \frac{M_n \times (y + 2z)}{146x + 163y + 180z} \quad (3)$$

where M_n is the number average molecular weight of HBPA, x is the content of dendritic units (molar mass: 146 g/mol), y is the content of linear units (molar mass: 163 g/mol), and z is the content of terminal units (molar mass: 180 g/mol).

The apparent molecular weight of HBPA measured by GPC is 26046 , and the degree of branching is 49.5% , the number of carboxyl groups contained in each macromolecule is 145 (Table S1, Fig. S5). The above results show that the carboxyl-terminated HBPA was successfully synthesized.

The carboxyl groups on HBPA can react with epoxy groups of EPI and EBN to form β -hydroxyester bonds via hot pressing. The low viscosity of HBPA is beneficial for uniform dispersion in the rubber matrix. The esterification reaction between EPI, EBN and HBPA has been proved by comparing the FTIR spectra of uncured and cured EB20 (Fig. 2d). For uncured EB20, the peaks at 875 and 1720 cm^{-1} are corresponded to epoxy groups and carbonyl in carboxyl groups. The peak of the epoxy groups at 875 cm^{-1} of cured EB20 disappeared, and the peak corresponding to the stretching vibration of -OH appeared at 3448 cm^{-1} , while the peak at 1720 cm^{-1} enhanced because of the formation of ester bonds. These results indicate that HBPA can consume the epoxy groups to form covalent cross-linking networks. The new peaks of ether bonds appearing between 1050 and 1110 cm^{-1} are assigned to the homopolymerization of epoxy groups [45].

After soaking samples in toluene for 72 h , the sample still did not dissolve and just swelled (Fig. S6), further illustrating the formation of cross-linking structure. According to the equilibrium swelling tests, as the EBN loading increased, the cross-linking density increased and the swelling ratio decreased (Table S2).

SEM was used to estimate the dispersion states of hBN and EBN in EPI. As shown in Fig. 3a and b, under the same loading fraction, BN aggregated together with poor dispersibility. In contrast, EBN dispersed uniformly in the EPI matrix (Fig. 3c and d), without obvious aggregations. This is because the hydrophilic component grafted KH-560 is beneficial to enhance the compatibility between rubber and EBN. Furthermore, the carboxyl groups on HBPA react with epoxy groups on the EBN and EPI to form β -hydroxyester bonds, which not only enhanced the interaction between EBN and EPI matrix, but also avoided the thermodynamically favorable re-aggregation of EBN during sample preparation [46].

3.2. Mechanical properties of composites

Dynamic mechanical properties of the composites under different EBN loading were studied by DMA test. As shown in Fig. 4a, as the loading of EBN increase, the storage modulus (E') increases, while the peak value of $\tan\delta$ decreases (Fig. 4b). Similar to most fillers [33,47,48], BN can restrict the movement of chain segments so they do not take part in bulk relaxation, and covalent bonds at the interface enhances this restriction, increasing E' and decreasing the peak value of $\tan\delta$.

Fig. 4c shows the stress-strain curves of EB composites, and Table S3 summarizes their mechanical properties. By changing the load of EBN, the mechanical properties of sample can be controlled easily. As the EBN loading increases, the tensile strength of the composite increases, and the elongation at break decreases. EB10 exhibits typical elastic behavior but other samples show different shapes. This can be attributed to the fact that with the loading of EBN, the cross-linking density of the sample increases, resulting in a higher initial modulus of the material (Table S3), so the strength can rise rapidly within a small range of initial stretching. In particular, EB50 exhibited plastic behavior with yield stress because of its glass transition temperature (T_g) rising above room temperature (Fig. 4b, Table S3). Compared with other reported vitrimer elastomers, EB samples have better or comparable mechanical properties (Table S4). The strong mechanical properties are attributed to the uniform dispersion of EBN and the formation of covalent bonds between the interfaces of fillers and matrix. We further compared the effects of carboxyl-terminated polyamides with different structures as cross-linking agents on the properties of the materials. The linear polyamide (PA-66) and hyperbranched aliphatic polyamide (HBP-aliphatic) with terminal carboxyl groups were synthesized according to the literature, and the corresponding structures were characterized by FTIR and ^1H NMR (Fig. S7). The carboxyl content of PA-66 was titrated by KOH, and PA-66 with the same amount of carboxyl groups was added instead of HBPA while keeping other conditions unchanged. When linear polyamides were used as cross-linking agents, the elongation at break and ultimate strength of the samples are significantly reduced (Fig. S8a). This can be attributed to two reasons. First, each linear polyamide molecule has only one or two carboxyl ends, while hyperbranched polymers have abundant carboxyl ends. In order to achieve the same carboxyl content as the hyperbranched polyamide, 32.5 phr linear PA-66 must be added to achieve the carboxyl content equivalent to 10 phr HBPA, which is easy to introduce defects. In addition, the dispersion of linear polyamides is much more uneven in the matrix than that of low-viscosity hyperbranched polyamides, resulting in uneven cross-linking distribution. The hyperbranched aliphatic polyamides with carboxyl ends have also been synthesized by the copolymerization of ethylenediamine and ethylenediaminetetraacetic acid, with the similar carboxyl content as HBPA for comparison, and the structure of which can be confirmed by FTIR and ^1H NMR (Fig. S7b, e). As shown in Fig. S8b, under the same conditions, hyperbranched aliphatic

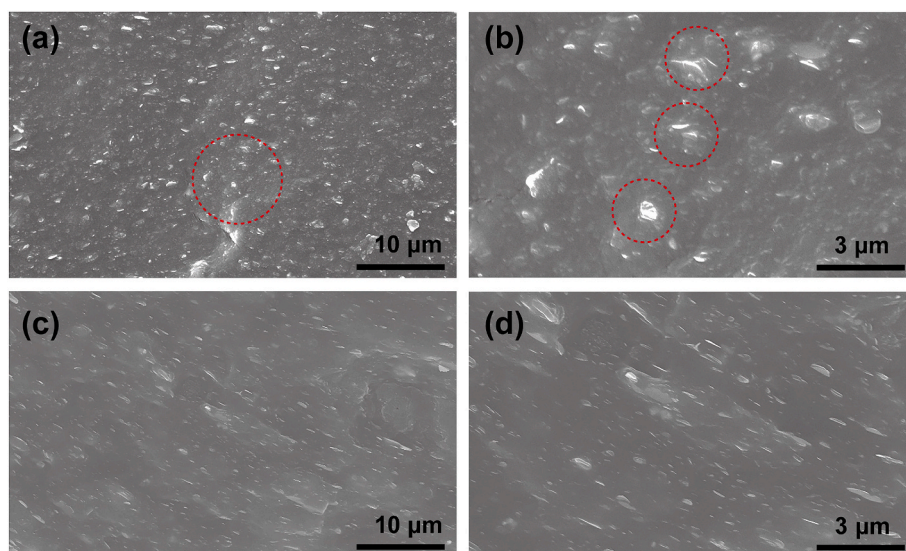


Fig. 3. SEM images of samples containing 40 phr (a, b) BN and (c, d) EBN.

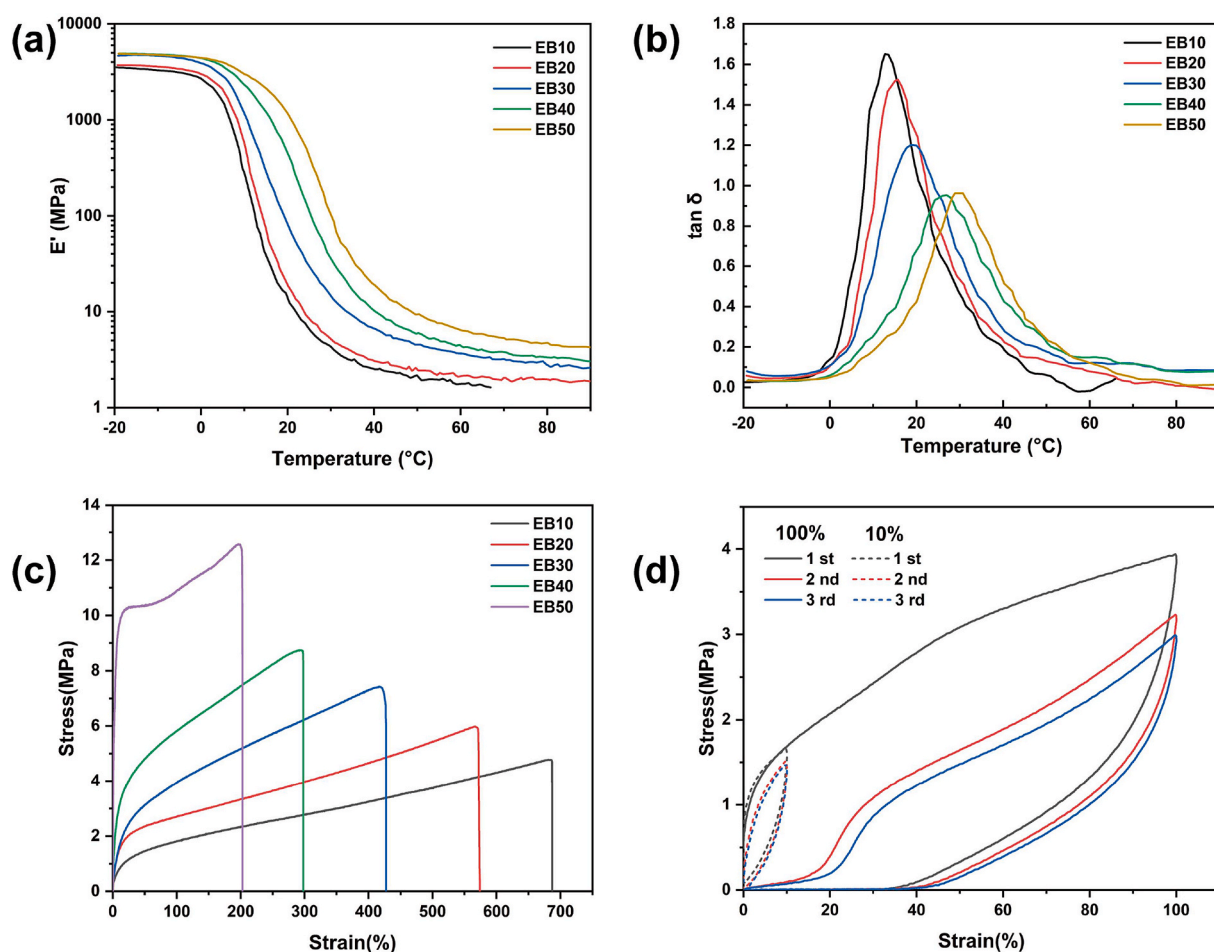


Fig. 4. (a) Storage modulus and (b) loss factor of EB samples. (c) Stress–strain curves of EB samples. (d) Loading–unloading curves of EB30.

polyamides can obtain higher elongation at break as crosslinking agents, and exhibit typical elastic deformation at the same time, but the corresponding ultimate strength has decreased. This is because the aromatic structure of HBPA has greater steric hindrance and more significant restriction on chain segment motion [49]. It is known that the

construction of structures containing long and short chains in composites is an effective “sacrificial bond” mechanism [50]. In the EB samples, HBPA can connect EPI matrix with EBN. The long chain maintains the elasticity and structure of the composites. Shorter chains may be formed between adjacent EBN or EPI segments. Under the action of external

forces, short chains preferentially break to dissipate energy and reinforce samples. Cyclic stretching experiments can well support this mechanism. Taking EB30 as an example (Fig. 4d), when stretched to 10%, it can almost completely recover the first cycle curve. However, when the strain is 100%, a significant hysteresis is observed, which means that a large amount of energy is dissipated. In addition, the sample failed to recover original length after unloading the stress and showed significant residual strain. After being placed for 10 min before reloading, the residual strain disappeared partially but still could not return to the first loading curve, which shows that the short chain broke irreversibly in the first cycle due to the high strain.

3.3. Network rearrangement of EB composites

At high temperatures, EB samples can rearrange the topology through dynamic transesterification of β -hydroxy ester bonds (Fig. 5a). The stress relaxation behavior of EB30 at different temperatures was shown in Fig. 5b. Apparently, the stress decreases with time and the rate of relaxation accelerates with increasing temperature. This is because the samples are crosslinked by β -hydroxy ester bonds, so the relaxation process is mainly depended on ester exchange reaction rate, while higher temperatures can accelerate the exchange. The higher temperature is beneficial to the movement of rubber chain segments, thereby increasing the probability of ester bond collision. The time needed for relaxing 63% initial stress is defined as characteristic relaxation time (τ^*), which follows Arrhenius's law (Fig. S10). The calculated activation energy value is 106.2 kJ/mol, which is in line with the value reported by

Leibler et al. (80–120 kJ/mol) [51,52]. Fig. 5c shows the stress relaxation of different EB samples with 2% constant deformation at 80 °C. All samples showed significant stress relaxation, and the relaxation rate decreased with increasing EBN loading. This is because higher cross-linking density networks require more exchange reactions to achieve topological rearrangement, and more EBN will also limit the mobility of the rubber segments, hinder the transesterification reaction, and prolong the relaxation time. The creep behavior of all samples was tested at 80 °C with a constant stress of 0.2 MPa. The strain of all samples increased almost linearly with time under test conditions, while the slope of the curve decreased with increasing EBN loading (Fig. S11).

3.4. Thermal properties of EB composites

BN has great application prospects in thermally conductive. Fig. 6a shows the cross-plane thermal conductivity (λ) of samples with different EBN loading fractions. Thermal conductivity of all samples increased with EBN loading. This is because increasing the EBN allows more crystal structure and specific surface area in the composites to provide channels for phonon transmission. To further compare the effect of BN modification on thermal conductivity, the thermal conductivity of samples with the same loading of BN were also tested. Obviously, composites with EBN added at the same filler content show higher thermal conductivity. EB50 samples have the highest thermal conductivity of 0.51 W/mK. The thermal conductivity of the EB50 sample is 4.6 times as much as pure EPI (0.11 W/mK). There are two reasons for the increase in thermal conductivity. The main reason is that good

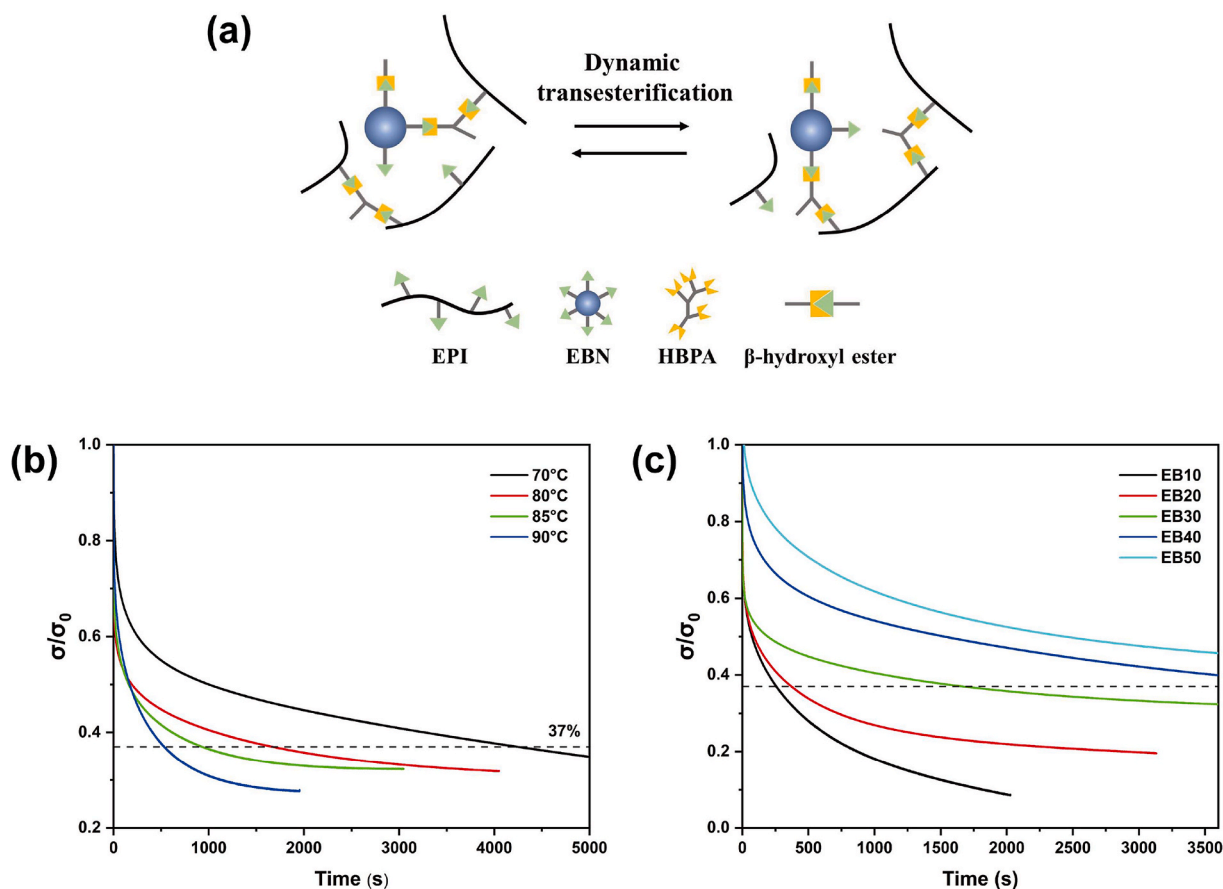


Fig. 5. (a) Schematic diagram of the topology rearrangement through transesterification. (b) Stress relaxation for EB30 sample at different temperatures. (c) Stress relaxation for EB samples at 80 °C.

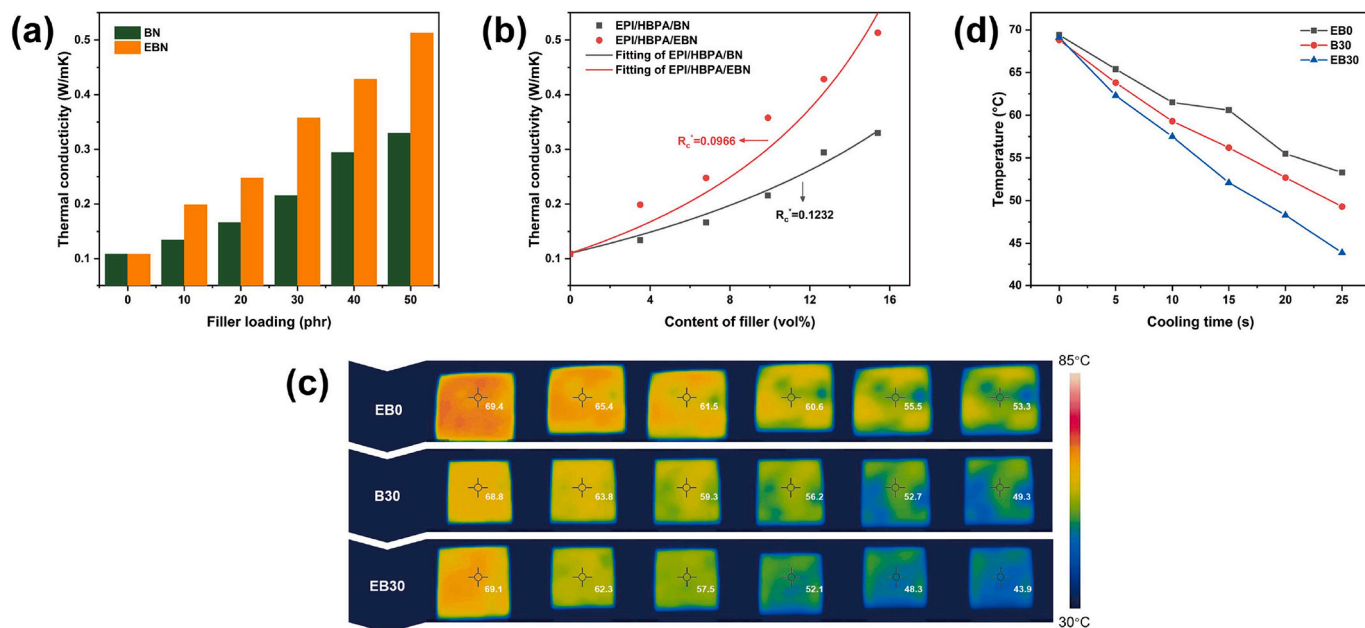


Fig. 6. (a) The thermal conductivity of composites filled with different BN and EBN loading. (b) Fitting experimental thermal conductivity by modified Hashin-shtrikman model. (c) Infrared thermal images and (d) corresponding temperature changes vs time of EB0, B30, and EB30.

interfacial interactions reduce the interface thermal resistance of composites. EBN linked EPI through β -hydroxyester bonds, which is beneficial to reduce phonon scattering, extend the average free path of the phonon, reduce Kapitza resistance, and promote phonon transmission [53]. Secondly, EBN uniformly dispersed in the rubber matrix. In contrast, due to poor interfacial interactions, aggregates and cracks exist in the composites filled with BN, and the interface thermal resistance increases, leading to a lower thermal conductivity. Wu et al. [54] increased the thermal conductivity of epoxy resin by 390% by fixing reduced graphene oxide on the surface of boron nitride. Yang et al. [55] deposited polydopamine on the surface of boron nitride and then grafted siloxane to increase the thermal conductivity of natural rubber by 300%. Compared to these excellent strategies, our work also achieved better or comparable high enhancement efficiency (360%) through simple modification steps. The results are listed in Table S5. Polyamides with different structures as crosslinking agents also have a certain impact on the thermal conductivity of the materials. Compared with hyperbranched aromatic polyamides, when linear polyamides are used as crosslinking agents, the samples display obvious defects and agglomerations in the fracture surface (Fig. S9), which is not conducive to heat transfer, resulting in an increase of thermal resistance and decrease of the thermal conductivity (Fig. S8c). When the samples were cross-linked by hyperbranched aliphatic polyamides instead of hyperbranched aromatic polyamides, the thermal conductivity decreased slightly, which may be due to the aromatic structure of HBPA, that is more conducive to phonon propagation (Fig. S8d) [56]. On the other hand, the loading of HBPA in the sample is small, and the content of EBN is the main factor affecting the thermal conductivity of the samples.

To further explain the influence of BN modification on the interfacial thermal resistance, we used modified Hashin-shtrikman model to evaluate the thermal resistance of composites [57,58].

$$\frac{\lambda_{eff}}{\lambda_m} = \frac{1 + 2k\sum_{i=1}^n E_i V_i}{1 - k\sum_{i=1}^n E_i V_i} \quad (4)$$

λ_{eff} is the experimental thermal conductivity of EB samples, λ_m is the thermal conductivity of EPI, n is the number of filler types, V_i is the filler volume fraction, and k is a coefficient related to the total thermal resistance of the composites. Eq (5) and Eq (6) are two empirical formulas for k are as follows:

$$K = 13.3347 \exp(-13.2701 R_C^*) \quad (5)$$

$$E_i = \frac{\frac{\lambda_i}{\lambda_m} - 1}{\frac{\lambda_i}{\lambda_m} + 1} \quad (6)$$

R_C^* is the total thermal resistance of composites. The relationship between filler volume fraction V_i and mass fraction wt is as follows:

$$V_i = \frac{1}{1 + \frac{(1-wt)/wt}{\rho_m/\rho_i}} \quad (7)$$

As shown in Fig. 6b, the total thermal resistance (R_C^*) of EPI/HBPA/BN is 0.1232, which is higher than that of EB composites (0.0966). It shows that compared with BN, EBN have lower thermal resistance. These results indicate that the surface modification of boron nitride and the covalent bonding between the filler and the matrix are beneficial to improve the thermal conductivity of the composite.

To study the thermal response of EB samples, infrared thermal imaging technology was used to record the surface temperature changes of the samples with time (Fig. 6c). The samples were put in an oven at 70 °C for 30 min. After the temperature was equilibrated, the samples were put on the stainless-steel plate, and the surface temperature was recorded every 5 s by infrared thermography. The surface temperature of EB30 decreased by 25 °C within 25s, while B30 (composites contain 30 phr BN) and EB0 (composites contain 0 phr BN) decreased by 19 °C and 16 °C, respectively (Fig. 6d). This trend is in line with the experimental λ value. Increasing the BN loading fraction can improve the thermal conductivity of samples. In addition, covalent cross-linking at the interface can reduce the thermal resistance between EBN and EPI interface and increase the thermal conductivity. The enhancement of interfacial effects is also manifested in the improvement of the thermal stability of samples (Fig. S12). The initial degradation temperature of EB samples is higher than 250 °C, indicating that the networks are thermally stable during high-temperature processing.

3.5. Reshaping and recycling of EB composites

As the EB samples have the characteristics of vitrimer, that is, the relationship between viscosity and temperature gradually changes

according to Arrhenius's law. Therefore, complex objects can be easily obtained by processing at 160 °C without molds and precise temperature control, and the material structure integrity is not affected. As shown in Fig. 7a, the EB samples can be simply processed at 160 °C to obtain permanently deformed elastomers.

Through the transesterification reactions, the EB samples can change their network topology to release the stress, which makes the EB samples recyclable. As a proof of concept, the coherent EB samples were obtained by pulverizing and re-moulding at 160 °C for 30 min, which proved the recyclability of EB samples (Fig. 7b). Moreover, the FTIR spectrum of the recovered samples (Fig.S13) almost coincides with that of the original sample, indicating that the network structure did not change significantly during reprocessing. We also compared the effect of linear structure of carboxy-terminal polyamide on reprocessing. As shown in Fig. S8e, when the linear polyamides were used as the crosslinking agents, the sample has a lower recovery efficiency, which is related to the poor dispersion of the linear polyamide. As shown in Fig. 7c, most of the initial mechanical properties of all samples can be recovered, indicating that covalent cross-linked rubber composites have excellent recyclability. Taking EB20 as an example, the stress-strain curves before and after recovery almost coincides even after two recycling cycles (Fig. 7d). However, with the increase of EBN load, the recovery rates of tensile strength and elongation at break decreases (Fig. 7c and S14). Although more β -hydroxyester bonds can be formed by adding more EBN, the chain movement and transesterification reaction are limited due to the increase of the crosslink density and the large volume fraction of the filler. In addition, we also synthesized an amino-terminated hyperbranched polyamide (HBPA-NH₂) with the same structure as HBPA for comparison. The structure of HBPA-NH₂ was characterized by FTIR and ¹H NMR (Fig. S7c, f). The covalently cross-linked samples (EPI/HBPA-NH₂/EBN) can be obtained through the reactions of amino groups on HBPA-NH₂ with epoxy groups, with other conditions unchanged. However, after being divided into small pieces, the cross-

linked sample such as EPI/HBPA-NH₂/EB20 cannot be reshaped by hot pressing, indicating that the β -hydroxy transesterification reaction plays an important role for the recyclability of the sample (Fig. S15).

4. Conclusions

In summary, EBN and HBPA assembled recyclable polyisoprene vitrimer with robust mechanical properties, high thermal conductivity, excellent recyclability and remoldability was achieved. The carboxyl-terminated HBPA was used as cross-linking agents, and reacted with epoxy groups on EBN and EPI at high temperature to construct dynamic cross-linking network with β -hydroxyester bonds. When the loading of EBN is 50 phr, the maximum tensile strength is 12.6 Mpa, and the thermal conductivity value of the corresponding composites is 0.51 W/mK, which is 4.6 times than that of pure EPI (0.11 W/mK). In addition, comparing with other BN-based thermal-conducting rubber composites, EB samples can be dynamically shuffled through transesterification reactions to rearrange the network topology, achieving recycling and remolding. EB samples can be easily processed into complex geometric shapes by heating and stress relaxation. And the EB composites can recover most of their mechanical properties through transesterification reactions. Considering the abundance of various rubbers and thermally conductive fillers, we envision this strategy can be used to develop robust vitrimer materials with high thermal conductivity and recyclable elastomers, showing huge potential applications in the field of flexible electronic substrates, thermal management materials, etc.

CRediT authorship contribution statement

Lingyun Huang: Conceptualization, Methodology, Investigation, Data curation, Writing - original draft, Writing - review & editing. **Yinxin Yang:** Validation, Visualization. **Ruiyao Wu:** Validation, Resources. **Weifeng Fan:** Methodology, Resources. **Quanquan Dai:**

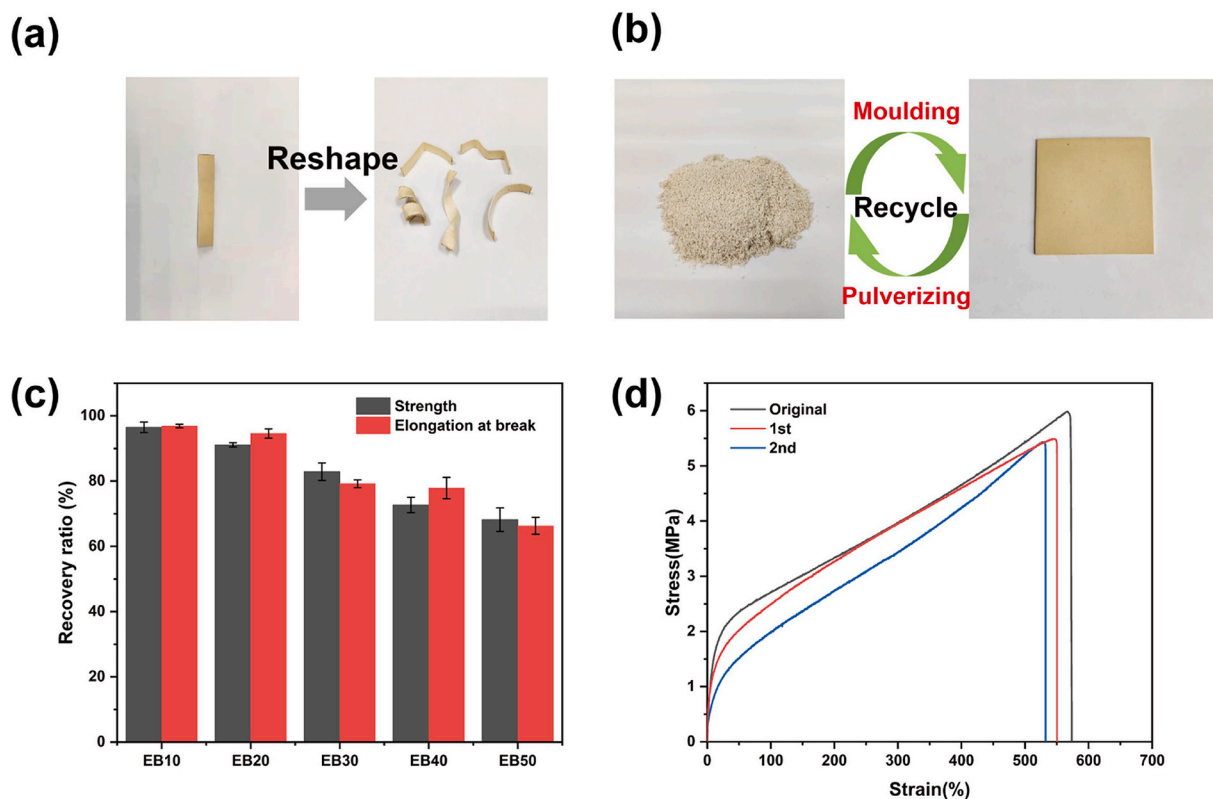


Fig. 7. (a) Reshaping of EB composite at 160 °C to obtain various shapes. (b) Recycling of EB samples. (c) Recovery ratio of mechanical properties of EB samples after recycling. (d) The typical tensile curves of the EB20 after multiple recycle.

Resources. **Jianyun He:** Conceptualization, Methodology, Project administration. **Chenxi Bai:** Supervision, Funding acquisition.

Declaration of competing interest

The authors declare that they have no known competing financial interests or personal relationships that could have appeared to influence the work reported in this paper.

Acknowledgment

This work was supported by the National Natural Science Foundation of China (No. 51873203), Key Projects of Jilin Province Science and Technology Development Plan (No. 20180201087GX, 20200401042GX, 20200401041GX), the Project of Talent Development Fund of Jilin Province (NO. Y9390002), and Special Fund Supported Project for High-tech Industrialization of Science and Technology Cooperation between Jilin Province and the Chinese Academy of Sciences (2019SYHZ0003).

Appendix A. Supplementary data

Supplementary data to this article can be found online at <https://doi.org/10.1016/j.polymer.2020.122964>.

References

- [1] M. Donnay, S. Tzavalas, E. Logakis, Boron nitride filled epoxy with improved thermal conductivity and dielectric breakdown strength, *Compos. Sci. Technol.* 110 (2015) 152–158.
- [2] X. Huang, C. Zhi, P. Jiang, D. Golberg, Y. Bando, T. Tanaka, Polyhedral oligosilsesquioxane-modified boron nitride nanotube based epoxy nanocomposites: an ideal dielectric material with high thermal conductivity, *Adv. Funct. Mater.* 23 (2013) 1824–1831.
- [3] Z. Kuang, Y. Chen, Y. Lu, L. Liu, S. Hu, S. Wen, Y. Mao, L. Zhang, Fabrication of highly oriented hexagonal boron nitride nanosheet/elastomer nanocomposites with high thermal conductivity, *Small* 11 (2015) 1655–1659.
- [4] M. Inagaki, Y. Kaburagi, Y. Hishiyama, Thermal management material: graphite, *Adv. Eng. Mater.* 16 (2014) 494–506.
- [5] C.P. Feng, S.S. Wan, W.C. Wu, L. Bai, R.Y. Bao, Z.Y. Liu, M.B. Yang, J. Chen, W. Yang, Electrically insulating, layer structured SiR/GNPs/BN thermal management materials with enhanced thermal conductivity and breakdown voltage, *Compos. Sci. Technol.* 167 (2018) 456–462.
- [6] X. Xu, T. Yu, Z. Bi, W. Ma, Y. Li, Q. Peng, Realizing over 13% efficiency in green-solvent-processed nonfullerene organic solar cells enabled by 1,3,4-thiadiazole-based wide-bandgap copolymers, *Adv. Mater.* 30 (2018) 1703973.
- [7] Y. Yao, J. Sun, X. Zeng, R. Sun, J.-B. Xu, C.-P. Wong, Construction of 3D skeleton for polymer composites achieving a high thermal conductivity, *Small* 14 (2018) 1704044.
- [8] E. Trovatti, T.M. Lacerda, A.J.F. Carvalho, A. Gandini, Recycling tires? Reversible crosslinking of poly(butadiene), *Adv. Mater.* 27 (2015) 2242–2245.
- [9] J. Han, G. Du, W. Gao, H. Bai, An anisotropically high thermal conductive boron nitride/epoxy composite based on Nacre-mimetic 3D network, *Adv. Funct. Mater.* 29 (2019) 1900412.
- [10] D. An, S. Cheng, Z. Zhang, C. Jiang, H. Fang, J. Li, Y. Liu, C.-P. Wong, A polymer-based thermal management material with enhanced thermal conductivity by introducing three-dimensional networks and covalent bond connections, *Carbon* N. Y. 155 (2019) 258–267.
- [11] L. Fang, W. Wu, X. Huang, J. He, P. Jiang, Hydrangea-like zinc oxide superstructures for ferroelectric polymer composites with high thermal conductivity and high dielectric constant, *Compos. Sci. Technol.* 107 (2015) 67–74.
- [12] J.-W. Zha, Y.-H. Zhu, W.-K. Li, J. Bai, Z.-M. Dang, Low dielectric permittivity and high thermal conductivity silicone rubber composites with micro-nano-sized particles, *Appl. Phys. Lett.* 101 (2012), 062905.
- [13] W. Dai, J. Yu, Y. Wang, Y. Song, F.E. Alam, K. Nishimura, C.-T. Lin, N. Jiang, Enhanced thermal conductivity for polyimide composites with a three-dimensional silicon carbide nanowire/graphene sheets filler, *J. Mater. Chem. A* 3 (2015) 4884–4891.
- [14] L. Yin, X. Zhou, J. Yu, H. Wang, C. Ran, Fabrication of a polymer composite with high thermal conductivity based on sintered silicon nitride foam, *Compos. Part A Appl. Sci. Manuf.* 90 (2016) 626–632.
- [15] W. Jiajun, Y. Xiao-Su, Effects of interfacial thermal barrier resistance and particle shape and size on the thermal conductivity of AlN/PI composites, *Compos. Sci. Technol.* 64 (2004) 1623–1628.
- [16] Y. Jiang, X. Shi, Y. Feng, S. Li, X. Zhou, X. Xie, Enhanced thermal conductivity and ideal dielectric properties of epoxy composites containing polymer modified hexagonal boron nitride, *Compos. Part A Appl. Sci. Manuf.* 107 (2018) 657–664.
- [17] T. Kashiwagi, E. Grulke, J. Hilding, K. Groth, R. Harris, K. Butler, J. Shields, S. Kharchenko, J. Douglas, Thermal and flammability properties of polypropylene/carbon nanotube nanocomposites, *Polymer* 45 (2004) 4227–4239.
- [18] J.R. Potts, D.R. Dreyer, C.W. Bielawski, R.S. Ruoff, Graphene-based polymer nanocomposites, *Polymer* 52 (2011) 5–25.
- [19] C. Tan, X. Cao, X.-J. Wu, Q. He, J. Yang, X. Zhang, J. Chen, W. Zhao, S. Han, G.-H. Nam, M. Sindoro, H. Zhang, Recent advances in ultrathin two-dimensional nanomaterials, *Chem. Rev.* 117 (2017) 6225–6331.
- [20] J. He, L. Huang, Y. Yang, Y. Qi, L. Cui, Q. Dai, C. Bai, High Tg and thermostable phytic Acid–Cured polynorbornene-based polymer by a Palladium(II) complex bearing iminophenyl oxazolinyphenylamines ligand, *Polymer* 172 (2019) 196–204.
- [21] J. Gu, X. Meng, Y. Tang, Y. Li, Q. Zhuang, J. Kong, Hexagonal boron nitride/polymethyl-vinyl siloxane rubber dielectric thermally conductive composites with ideal thermal stabilities, *Compos. Part A Appl. Sci. Manuf.* 92 (2017) 27–32.
- [22] J. Yu, X. Huang, C. Wu, X. Wu, G. Wang, P. Jiang, Interfacial modification of boron nitride nanoplatelets for epoxy composites with improved thermal properties, *Polymer* 53 (2012) 471–480.
- [23] T. Morishita, N. Takahashi, Highly thermally conductive and electrically insulating polymer nanocomposites with boron nitride nanosheet/ionic liquid complexes, *RSC Adv.* 7 (2017) 36450–36459.
- [24] K. Kim, M. Kim, Y. Hwang, J. Kim, Chemically modified boron nitride-epoxy terminated dimethylsiloxane composite for improving the thermal conductivity, *Ceram. Int.* 40 (2014) 2047–2056.
- [25] Z.P. Zhang, M.Z. Rong, M.Q. Zhang, Polymer engineering based on reversible covalent chemistry: a promising innovative pathway towards new materials and new functionalities, *Prog. Polym. Sci.* 80 (2018) 39–93.
- [26] D. Montarnal, M. Capelot, F. Tournilhac, L. Leibler, Silica-like malleable materials from permanent organic networks, *Science* 334 (80-) (2011) 965–968.
- [27] J. Dahlke, S. Zechel, M.D. Hager, U.S. Schubert, How to design a self-healing polymer: general concepts of dynamic covalent bonds and their application for intrinsic healable materials, *Adv. Mater. Interfaces* 5 (2018) 1800051.
- [28] G.M. Scheutz, J.J. Lessard, M.B. Sims, B.S. Sumerlin, Adaptable crosslinks in polymeric materials: resolving the intersection of thermoplastics and thermosets, *J. Am. Chem. Soc.* 141 (2019) 16181–16196.
- [29] T. Liu, B. Zhao, J. Zhang, Recent development of repairable, malleable and recyclable thermosetting polymers through dynamic transesterification, *Polymer* 194 (2020) 122392.
- [30] F. Ji, X. Liu, D. Sheng, Y. Yang, Epoxy-vitrimer composites based on exchangeable aromatic disulfide bonds: reprocessability, adhesive, multi-shape memory effect, *Polymer* 197 (2020) 122514.
- [31] M.M. Obadia, B.P. Mudraboyina, A. Serghei, D. Montarnal, E. Drockenmüller, Reprocessing and recycling of highly cross-linked ion-conducting networks through transalkylation exchanges of C–N bonds, *J. Am. Chem. Soc.* 137 (2015) 6078–6083.
- [32] Y.-X. Lu, F. Tournilhac, L. Leibler, Z. Guan, Making insoluble polymer networks malleable via olefin metathesis, *J. Am. Chem. Soc.* 134 (2012) 8424–8427.
- [33] Y. Liu, Z. Tang, Y. Chen, S. Wu, B. Guo, Programming dynamic imine bond into elastomer/graphene composite toward mechanically strong, malleable, and multi-stimuli responsive vitrimer, *Compos. Sci. Technol.* 168 (2018) 214–223.
- [34] O.R. Cromwell, J. Chung, Z. Guan, Malleable and self-healing covalent polymer networks through tunable dynamic boronic ester bonds, *J. Am. Chem. Soc.* 137 (2015) 6492–6495.
- [35] W.-X. Liu, C. Zhang, H. Zhang, N. Zhao, Z.-X. Yu, J. Xu, Oxime-based and catalyst-free dynamic covalent polyurethanes, *J. Am. Chem. Soc.* 139 (2017) 8678–8684.
- [36] S.H. Cho, H.M. Andersson, S.R. White, N.R. Sottos, P.V. Braun, Polydimethylsiloxane-based self-healing materials, *Adv. Mater.* 18 (2006) 997–1000.
- [37] X. Yang, Y. Guo, X. Luo, N. Zheng, T. Ma, J. Tan, C. Li, Q. Zhang, J. Gu, Self-healing, recoverable epoxy elastomers and their composites with desirable thermal conductivities by incorporating BN fillers via in-situ polymerization, *Compos. Sci. Technol.* 164 (2018) 59–64.
- [38] T. Liu, Y. Nie, R. Chen, L. Zhang, Y. Meng, X. Li, Hyperbranched polyether as an all-purpose epoxy modifier: controlled synthesis and toughening mechanisms, *J. Mater. Chem. A* 3 (2015) 1188–1198.
- [39] G. Zhao, F. Zhang, Y. Wu, X. Hao, Z. Wang, X. Xu, One-Step exfoliation and hydroxylation of boron nitride nanosheets with enhanced optical limiting performance, *Adv. Opt. Mater.* 4 (2016) 141–146.
- [40] V.A. Tomaz, A.F. Rubira, R. Silva, Solid-state polymerization of EDTA and ethylenediamine as one-step approach to monodisperse hyperbranched polyamides, *RSC Adv.* 6 (2016) 40717–40723.
- [41] Y. Yu, M.Z. Rong, M.Q. Zhang, Grafting of hyperbranched aromatic polyamide onto silica nanoparticles, *Polymer* 51 (2010) 492–499.
- [42] R.J. Angelo, H. Miura, K.H. Gardner, D.B. Chase, A.D. English, Preparation and characterization of selectively isotopically labeled nylon 66 polymers, *Macromolecules* 22 (1989) 117–121.
- [43] S. Livi, E.P. Giannelis, An improved process for the surface modification of SiO₂ nanoparticles, *Green Chem.* 14 (2012) 3013.
- [44] D. Halter, A. Burgath, H. Frey, Degree of branching in hyperbranched polymers, *Acta Polym.* 48 (1–2) (1997) 30–35.
- [45] C. Ding, P.S. Shuttleworth, S. Makin, J.H. Clark, A.S. Matharu, New insights into the curing of epoxidized linseed oil with dicarboxylic acids, *Green Chem.* 17 (2015) 4000–4008.
- [46] Y. Liu, Z. Tang, Y. Chen, C. Zhang, B. Guo, Engineering of β -hydroxyl esters into elastomer-nanoparticle interface toward malleable, robust, and reprocessable vitrimer composites, *ACS Appl. Mater. Interfaces* 10 (2018) 2992–3001.

- [47] A. Legrand, C. Soulié-Ziakovic, Silica–epoxy vitrimer nanocomposites, *Macromolecules* 49 (2016) 5893–5902.
- [48] L. Cao, J. Fan, J. Huang, Y. Chen, A robust and stretchable cross-linked rubber network with recyclable and self-healable capabilities based on dynamic covalent bonds, *J. Mater. Chem. A* 7 (2019) 4922–4933.
- [49] M. Harada, D. Morioka, M. Ochi, Thermal and mechanical properties of tetra-functional mesogenic type epoxy resin cured with aromatic amine, *J. Appl. Polym. Sci.* 135 (2018) 46181.
- [50] Z. Tang, Y. Liu, B. Guo, L. Zhang, Malleable, mechanically strong, and adaptive elastomers enabled by interfacial exchangeable bonds, *Macromolecules* 50 (2017) 7584–7592.
- [51] F.I. Altuna, V. Pettarin, R.J.J. Williams, Self-healable polymer networks based on the cross-linking of epoxidised soybean oil by an aqueous citric acid solution, *Green Chem.* 15 (2013) 3360.
- [52] F.I. Altuna, C.E. Hoppe, R.J.J. Williams, Shape memory epoxy vitrimers based on DGEBA crosslinked with dicarboxylic acids and their blends with citric acid, *RSC Adv.* 6 (2016) 88647–88655.
- [53] C. Pan, K. Kou, Q. Jia, Y. Zhang, G. Wu, T. Ji, Improved thermal conductivity and dielectric properties of hBN/PTFE composites via surface treatment by silane coupling agent, *Compos. B Eng.* 111 (2017) 83–90.
- [54] K. Wu, C. Lei, W. Yang, S. Chai, F. Chen, Q. Fu, Surface modification of boron nitride by reduced graphene oxide for preparation of dielectric material with enhanced dielectric constant and well-suppressed dielectric loss, *Compos. Sci. Technol.* 134 (2016) 191–200.
- [55] D. Yang, Y. Ni, X. Kong, D. Gao, Y. Wang, T. Hu, L. Zhang, Mussel-inspired modification of boron nitride for natural rubber composites with high thermal conductivity and low dielectric constant, *Compos. Sci. Technol.* 177 (2019) 18–25.
- [56] J. Liu, R. Yang, Length-dependent thermal conductivity of single extended polymer chains, *Phys. Rev. B* 86 (2012) 104307.
- [57] I.L. Ngo, C. Byon, B.J. Lee, Analytical study on thermal conductivity enhancement of hybrid-filler polymer composites under high thermal contact resistance, *Int. J. Heat Mass Tran.* 126 (2018) 474–484.
- [58] I.-L. Ngo, S.V. Prabhakar Vattikuti, C. Byon, A modified Hashin-Shtrikman model for predicting the thermal conductivity of polymer composites reinforced with randomly distributed hybrid fillers, *Int. J. Heat Mass Tran.* 114 (2017) 727–734.